Rich-club network topology to minimize synchronization cost due to phase difference among frequency-synchronized oscillators

Takamitsu Watanabe [*1]

[1]*Department of Physiology, School of Medicine, The University of Tokyo, 7-3-1 Hongo, Bunkyo-ku, Tokyo 113-8656, Japan*

Abstract

As exemplified by power grids and large-scale brain networks, some functions of networks consisting of phase oscillators rely on not only frequency synchronization, but also phase synchronization among the oscillators. Nevertheless, even after the oscillators reach frequency-synchronized status, the phase synchronization is not always accomplished because the phase difference among the oscillators is often trapped at non-zero constant values. Such phase difference potentially results in inefficient transfer of power or information among the oscillators, and avoids proper and efficient functioning of the networks. In the present study, we newly define synchronization cost by using the phase difference among the frequency-synchronized oscillators, and investigate the optimal network structure with the minimum synchronization cost through rewiring-based optimization. By using the Kuramoto model, we demonstrate that the cost is minimized in a network with a rich-club topology, which comprises the densely-connected center nodes and low-degree peripheral nodes connecting with the center module. We also show that the network topology is characterized by its bimodal degree distribution, which is quantified by Wolfson's polarization index.

* takawatanabe-tky@umin.ac.jp

I. INTRODUCTION

As seen in power grids [1, 2] and networks of bursting neurons [3, 4], some functions of complex networks consisting of phase oscillators are based on not only synchronization of frequencies among the oscillators, but also synchronization of their phases. However, in general, the frequency synchronization is more achievable than the phase synchronization because the phase difference among the frequency-synchronized oscillators often falls into a non-zero constant. Such non-zero phase difference avoids proper and efficient functioning of the complex networks [1–6].

In power grids, alternating voltage of the power plants in the grids should be synchronized around a certain specific frequency (*e.g.,* 50 Hz in the most parts of Europe and 60 Hz in the north America) [1], and disruption of the frequency synchronization causes a blackout in a large area [1, 7]. In addition, the phases of the voltages of the power plants are also required to be synchronized. As discussed in Appendix A, the difference in the voltage phases among the power plants inevitably causes power loss that is consumed as heat in the power lines among the plants [1, 2]. In this sense, the phase difference in power grids can be regarded as synchronization cost. Considering recent growing environmental awareness and soaring global demand of natural resources [8, 9], it is necessary to reduce the synchronization cost due to the phase difference among the frequency-synchronized power plants.

In a large-scale brain network, some of its important functions are also based on not only frequency- but also phase- synchronization [3, 4, 10, 11]. A previous electrophysiological study has shown that spike activity recorded from monkeys' cortices exhibited phase synchronization in various frequency bands while the monkeys were conducting tasks that required integration of visual processing and motor responses [10]. In another careful electrophysiology study, Roelfsema and his colleagues recorded local field potentials (LFP) from the cerebral cortices of cats and revealed that phase synchronization between LFPs recorded in the visual and parietal cortices increased only when the cats focused their attention on the visual stimuli [12]. Other studies used electro-encephalogram to record human brain activity and found that the increase of phase synchronization in various frequency bands was associated with learning and perception of visual images of the humans [13, 14]. Furthermore, even in large-scale brain networks, such phase synchronization is thought to occur with zero time-lag [4, 12, 15]. As a whole, these researches have suggested that the phase synchronization in large-scale brain networks

has crucial functions such as integration of multiple information [3], neural communication [16], and spike-timing-dependent plasticity [4]. Actually, some types of the disruption of the synchronization are known to cause dysfunctions of memory learning [5] or psychiatric disorders [6]. Hence, it is to some extent reasonable to hypothesize that large-scale brain networks have a specific organization that minimizes phase differences among brain activity and makes it easy for the entire networks to reach phase synchronization.

These previous literatures indicate the importance of investigation of the optimal network topology that minimizes the phase difference among frequency-synchronized oscillators, which can be regarded as synchronization cost. However, to our knowledge, little is examined about this issue. Indeed, a series of previous literatures have investigated optimal network structures by introducing a different type of synchronization cost, which is needed to build or maintain the optimal network infrastructure [17, 18]. One of the studies regarded parameters related to coupling strength among oscillators as synchronization cost and demonstrated that homogeneous and uniform distribution of the coupling strength enhances the tendency of synchronization [17]. Another study employing the same definition of synchronization cost suggests that more heterogeneous network structures are necessary for simultaneous achievement of both the maximum synchronizability and minimum synchronization cost [18]. Another study also investigated the optimal distribution of coupling strength that increases synchronizability among Kuramoto oscillators [19]. However, these prior researches have not focused on synchronization cost due to phase difference. Consequently, despite a large amount of prior literatures on optimal conditions for synchrony in networks [20], it remains unclear about the optimal network structures that minimize synchronization cost due to phase difference among oscillators.

In the present study, therefore, we examine the optimal network topology to minimize the phase-difference-based synchronization cost. We take the following four steps:

(i) First, we define the synchronization cost, S_{ij}, due to the phase difference between the frequency-synchronized phase oscillators i and j in the Kuramoto model. We adopt the Kuramoto model because the model has been used as approximation of various systems including power grids [2, 21, 22] (Appendix B) and large-scale brain networks [23, 24].

(ii) Second, by using the definition, we numerically calculate the mean of synchronization cost, $\langle S \rangle$, in the entire network.

(iii) Third, by using a rewiring strategy [25], we show that "rich-club" network topology

[24, 26–28], which consists of densely inter-connected modules and peripheral low-degree nodes, has the minimum synchronization cost.

(iv) Finally, we characterize the rich-club network topology by quantifying the bimodality of the degree distribution of the network.

II. METHOD

A. Definition of synchronization cost

We first define synchronization cost due to phase difference in an unweighted and undirected network which is described by an adjacency matrix A and consists of N phase oscillators. A_{ij} is 1 when oscillators i and j are connected, and A_{ij} is 0 when they are not. According to the Kuramoto model, the phase of the oscillator i, θ_i, is described as

$$\dot{\theta}_i = \omega_i - \epsilon \sum_j A_{ij} \sin(\theta_i - \theta_j), \tag{1}$$

where ω_i is the natural frequency of the oscillator i and ϵ is a coupling strength. To reduce computational cost for the following rewiring-based optimization, we assume that ϵ is a constant for any combination of oscillators. In this Kuramoto model, the synchronization cost between oscillators i and j, S_{ij}, is defined in the basis of the phase difference between them as follows:

$$S_{ij} = (\theta_i - \theta_j)^2 . \tag{2}$$

Note that the synchronization cost is only defined after the network of the oscillators reaches a state of frequency synchronization. In power grids, the network consisting of power plants can be approximated by the Kuramoto model (Appendix B) and S_{ij} can be regarded as an index that is proportional to power loss due to difference in voltage phase between power plants i and j (Appendix A).

B. Estimation of the mean synchronization cost

In the basis of the definition of S_{ij}, we numerically estimate S_{ij} for each edge in the following four steps for a given network:

(i) We set normally-distributed $\{\omega_i\}$ for each node. It is because that previous studies on real networks such as power grids and brain networks have assumed that the natural frequencies of their belonging oscillators are symmetrically fluctuating around the averaged frequency [4, 22, 29].

(ii) In the basis of the Kuramoto model described in Eq. (1), we numerically estimate phases of the oscillators in a frequency-synchronized status, in which $\dot{\theta}_i$ becomes a common constant value, Ω, for any i.

(iii) In the frequency-synchronized status, each oscillator has a different specific phase, θ_i. Using the set of $\{\theta_i\}$, we then evaluate S_{ij} for each edge.

(iv) As described in (i), the set of the natural frequency, $\{\omega_i\}$, is fluctuating over time and, consequently, the S_{ij} is also fluctuating over time. Therefore, we repeat the procedure (i)-(iii) 200 times with different sets of $\{\omega_i\}$ and obtain 200 different sets of $\{S_{ij}\}$ for each edge. Then, we average the $\{S_{ij}\}$ over time, obtaining $\langle S_{ij}\rangle$ for each edge. Finally, we average the $\langle S_{ij}\rangle$ across edges, and obtain $\langle S\rangle$ for the entire network.

C. Rewiring-based optimization

To search for the optimal network topology with the least $\langle S\rangle$, we adopt the rewiring-based method that previous studies used to explore the network topology with the largest synchronizability [25]. We apply the following rewiring-based optimization procedure to a given connected network with N nodes and mean degree of $\langle k\rangle$: At each step, the number of rewired edges is randomly determined based on an exponential distribution. The set of edges to be rewired is also randomly chosen in a given network. After the rewiring, we estimate phases of the oscillators in a frequency-synchronized status and obtain $\langle S\rangle_{\text{updated}}$. The attempted rewiring is rejected if the updated network is disconnected. Otherwise, the rewiring is accepted if $\Delta\langle S\rangle = \langle S\rangle_{\text{updated}} - \langle S\rangle_{\text{initial}} < 0$, or with probability $p = \min(1, [1-(1-q)\Delta\langle S\rangle/T]^{1/(1-q)})$ where T is a temperature-like parameter and $q = -3$ [25]. The initial rewiring is conducted at $T = \infty$, and, after the first N rewiring, T is set as $(1-q)(\Delta\langle S\rangle)_{\max}$ where $(\Delta\langle S\rangle)_{\max}$ is the largest $\Delta\langle S\rangle$ in the first N rewiring trials. After that, T decreased 10% in every 10 rewiring trials. This estimation process iterated until there is no change in more than 50 successive rewiring steps. We apply this rewiring-based optimization to three different initial networks:

an Erdős-Rényi (ER) random model, Watts-Strogatz (WS) model [30], and a Barabási-Albert (BA) model [31] with $N = 50$ and $\langle k \rangle = 4$ [25]. In all the cases, the coupling strength, ϵ, is set to be 0.3. Each set of the natural frequencies of Kuramoto oscillators, $\{\omega_i\}$, is randomly chosen from the normal distribution with an average of 100π and a standard deviation of 1.

During the optimization, we trace the standard order parameter, r, and local synchoronizability, r_{local} [32], defined as follows:

$$re^{i\psi} = \frac{1}{N}\sum_j e^{i\theta_j}, \tag{3}$$

$$r_{\text{local}} = \frac{1}{2N_l}\sum_i \sum_{j\in\Gamma_i} \left| \lim_{\Delta t\to\infty} \frac{1}{\Delta t}\int_{t_r}^{t_r+\Delta t} e^{i[\theta_i(t)-\theta_j(t)]}dt \right|, \tag{4}$$

where N_l is the total number of edges, Γ_i is the set of neighbors of node i, and ψ is a global phase. Furthermore, after the optimization is completed, we compare the optimized networks derived from the different initial networks by estimating the following basic topological properties: mean of shortest path length [33], mean of clustering coefficient [30], mean of betweenness centrality [34], and degree correlation [34]. We conducted ten optimizations of ten different networks for each type of the initial networks, and averaged these basic properties.

- The shortest path length, ℓ_{ij}, is defined as the shortest distance between two nodes i and j [33]. The averaged shortest path length, $\langle \ell \rangle$, is defined as an average value of ℓ_{ij} over all the possible pairs of the nodes in the network.

- The clustering coefficient for node i, C_i, measures the local group cohesiveness [30], which is defined as the ratio of the number of links between the neighbors of node i and the maximum number of such links. We define the mean clustering coefficient, $\langle C \rangle$, as an average value over all the nodes.

- The betweenness centrality for node i, b_i, is defined as a number of shortest paths between pairs of nodes that pass through a given node [34]. We define the mean betweenness centrality, $\langle b \rangle$, as an average value over all the nodes.

- The degree correlation for a network is defined as the Pearson assortativity coefficient of the degrees, $r_{\text{assortative}}$ [34]. The coefficient enables us to quantify the preference for high-degree nodes to attach to other high-degree nodes. Networks with this preference show large $r_{\text{assortative}}$.

D. Estimation of rich-club coefficient

We estimate rich-club coefficient, $\Phi(k)$, for both the initial networks and optimized networks. According to the previous studies [24, 26–28], the rich-club coefficient for each degree k is calculated as follows:

$$\Phi(k) = \frac{2E_{>k}}{N_{>k}(N_{>k}-1)}, \tag{5}$$

where $E_{>k}$ represents the number of edges among $N_{>k}$ nodes that have more than k degrees. As in previous studies [24, 27, 28], we calculate normalized rich-club coefficients, $\Phi_{\mathrm{norm}}(k)$: First, for each of the networks, we compute 100 random networks with the same degree distribution by using the method used in previous studies [28, 35]. We then calculate the rich-club coefficient for each of the random networks. Next, for each level of k, $\Phi_{\mathrm{random}}(k)$ is estimated as an average rich-club coefficient over the 100 random networks. Using the averaged rich-club coefficient, we finally calculate the normalized rich-club coefficient as follows:

$$\Phi_{\mathrm{norm}}(k) = \frac{\Phi(k)}{\Phi_{\mathrm{random}}(k)}. \tag{6}$$

III. RESULTS

A. Rewiring-based optimization

Fig. 1 shows representative results of the rewiring-based optimizations. $\langle S \rangle$ decreased from approximately 6.5×10^{-2} to 4.5×10^{-2} even when the initial network structure was different. In all the initial networks, $\langle S \rangle$ reached a stable status after approximate 400 steps of rewiring. Strikingly speaking, we cannot guarantee that the optimal network was found, but this result suggests that a reasonably robust approximation of the optimal topology was obtained in this method.

During the optimization, the standard order parameter, r, was fluctuating just below 1 (a small panel in Fig. 1 A). The local synchronizability, r_{local}, showed the similar fluctuation below 1. Considering the previous studies on these parameters [32], these behaviors of r and r_{local} are thought to be related to the amount of the coupling strength, ϵ. The previous studies [32] have demonstrated that, when the coupling strength is more than 0.2, both of r and r_{local} reach a plateau that is near to 1 regardless of the network topology. In the present study, the coupling strength, ϵ, was set at 0.3 to achieve global synchronization and calculate $\langle S \rangle$. This relatively

large coupling strength could result in the saturation of the global and local order parameters during the optimization process.

Fig. 1 B shows that the optimized networks for the three different initial networks commonly exhibit a characteristic topology: the networks have a densely interconnected core nodes and low-degree peripheral nodes dangling the core module. The heterogeneous network features were also observed in the basic network properties in the optimized networks (Tab. I). Compared with the initial networks, the optimized networks tended to show larger averaged values of the shortest path length, $\langle \ell \rangle$, betweenness centrality, $\langle b \rangle$, and degree correlation, $r_{\text{assortative}}$. The averaged values of the clustering coefficients, $\langle C \rangle$, were smaller in the optimized networks. These results suggest that, through the optimization process, the network seems to enlarge its heterogeneity.

B. Rich-club organization

This heterogeneous network topology has been reported as "rich-club" organization in a series of previous theoretical and experimental studies [24, 26–28]. The prior literatures have characterized the organization by estimating normalized rich-club coefficients, $\Phi_{\text{norm}}(k)$, that are described in Eq. 6. If the network has rich-club organization, $\Phi_{\text{norm}}(k)$ should be more than 1, and increase monotonically as k increases.

Fig. 2 shows the comparison in $\Phi_{\text{norm}}(k)$ between the initial networks and optimized networks. To clarify the difference in the rich-club coefficients, we adopted as the initial networks larger networks than shown in Fig. 1 B (*i.e.,* $N = 100, \langle k \rangle = 10$). Before the optimization, $\Phi_{\text{norm}}(k)$ was not always larger than 1 and did not show monotonic increase along k, which is consistent with a previous study [27]. In contrast, in the optimized networks, the rich-club coefficients were larger than 1 in large k, and almost monotonically increased as k increased. These phenomena were observed commonly among the three different optimized networks. In addition to the appearance of the networks in Fig. 1 B, this estimation of $\Phi_{\text{norm}}(k)$ supports the notion that networks with the minimum or a very small amount of synchronization cost have a rich-club topology.

C. Bimodal Degree Distribution

As shown in Fig. 1 B, the rich-club network topology consists of high-degree central nodes and low-degree peripheral nodes. Therefore, we hypothesized that the topology can be characterized by a bimodal degree distribution. To test the hypothesis, we estimated Wolfson's polarization index, $\hat{P}$ [36]. The Wolfson's index for degree distribution is defined as:

$$\hat{P} = \frac{2\langle k \rangle}{m} \left(2 \left(\langle k \rangle_2 - \langle k \rangle_1 \right) - G \right), \tag{7}$$

where $\langle k \rangle$ is the mean of the degree, k_i, and m denotes the median of the degree. $\langle k \rangle_1$ and $\langle k \rangle_2$ are the mean values of $\{k_i \mid k_i < m\}$ and of $\{k_i \mid k_i \geq m\}$, respectively. G represents Gini inequality index, which is defined as $G = \frac{1}{2\langle k \rangle} \sum_{i=1}^{N} \sum_{j=1}^{N} \mid k_i - k_j \mid$. This Wolfson's polarization index shows the extent of the bimodality of the distribution. If the distribution is completely the same as a uniform distribution, the $\hat{P}$ is 0. If the half of population has nothing and the other half shares everything, the $\hat{P}$ reaches a maximum, 0.25. In the present case, larger $\hat{P}$ indicates that the network has a more bimodal and bipolarized degree distribution.

We estimated $\hat{P}$ during the rewiring-based optimization. Because $\hat{P}$ can be calculated more accurately for networks with more nodes, we used the BA model with $N = 100$ and $\langle k \rangle = 4$ as an initial network for the optimization. As a result, in the course of the above-mentioned optimization, $\langle S \rangle$ decreased during the rewiring-based optimization (Fig. 3A). Meanwhile, as $\langle S \rangle$ decreased, $\hat{P}$ increased (Fig. 3B). Actually, the degree distribution changed from a power-law distribution (Fig. 3C) to a bimodal distribution (Fig. 3D). This relation was also observed for different initial networks (*e.g.,* ER model). This correlation supports the hypothesis that rich-club network with small $\langle S \rangle$ can be characterized by its bimodal degree distribution.

IV. DISCUSSION

The present study introduced synchronization cost based on phase difference among frequency-synchronized oscillators. Using the rewiring-based optimization [25, 37], we showed that the synchronization cost is minimized in a rich-club network topology. Furthermore, we demonstrated that the network topology can be characterized by the bimodality of its degree distribution.

The concept of synchronization cost is not a novel idea of the present study. As described in Sec. I, a line of previous studies have investigated a different type of synchronization cost,

which is based on coupling strength [17–19]. Whereas the present synchronization cost due to phase difference can be regarded as dynamic cost per unit time, the cost based on coupling strength can be considered as static cost that is related to building and maintaining of network infrastructures. Interestingly, the optimal network topology with the least cost depends on which of the two types of synchronization cost we adopt. The optimal networks for the synchronization cost based on coupling strength often show more homogeneous properties [17] than those for the other synchronization cost. The homogeneity of networks is desired to enhance synchronizability [25, 38]. Therefore, it may be necessary to investigate what network structures balance these two types of synchronization cost.

The present synchronization cost in the present study can be another concept of load assigned to edge in a complex network. Previous studies used edge-betweenness as edge load [39, 40], which is useful in various situations from human interaction [40] to data transmission in computer networks [39]. However, because the edge betweenness does not consider synchrony in networks, its properties have evident difference from those of the synchronization cost. For example, as shown in the following approximation in Eq. (9), the synchronization cost is lower between high degree nodes, and higher between low degree nodes. In contrast, the edge betweenness tends to be higher in edges bridging high degree nodes and be lower in edges bridging low degree nodes. These distinct properties suggest the possibility that the synchronization cost can be another concept of edge load.

The synchronization cost in the present study, S_{ij}, has a mathematical expression similar to that for local synchronizability, r_{local} [32]. However, the two parameters focus on different phases of synchronization in complex networks. The local synchronizability enables us to quantify the local construction of the synchronization pattern. Therefore, it is useful to investigate properties of networks that are not yet fully synchronized. In contrast, the synchronization cost in the present study can be only estimated in fully-synchronized networks. Therefore, in the present study, we used a relatively large coupling strength, and achieved full synchronization throughout the optimizations. As a result, in the present study, the local synchronizability was always saturated.

Although the present study did not adopt models specific to any real networks, the findings may help understanding large-scale brain networks. Recently, a few studies have reported the existence of the rich-club organization in the large-scale brain networks. A previous empirical study has demonstrated the existence of the rich-club organization in the human brain [28].

Another study has investigated the anatomical connectivity in the cerebral cortex of cats and has showed that rich-club organization controls the dynamic transition of synchronization in the brain [24]. A recent review has suggested that the organization is a cost-effective network topology for the brain networks, which are required to be adapted to various cognitive functions [41]. In addition to the context of cost-effectiveness, the rich-club network topology is thought to be robust to random attacks [42]. This previous study has analytically and numerically demonstrated that networks are robust to random attacks when they have highly-interconnected hub modules and peripheral nodes (*leaf* nodes) with a single edge. This network topology has bimodal degree distribution and shows rich-club organization. Considering these prior literatures, it is suggested that the rich-club organization is beneficial for the large-scale brain networks to efficiently and robustly maintain its wide range of functions based on synchronization.

Through a relatively simple calculation, we can discuss the analytical interpretation on the reasons why the rich-club topology appears after the rewiring-based optimization. Using mean-field approximation, the Eq. (1) in the frequency-synchronized status can be described as $\Omega = \omega_i - \epsilon k_i \sin(\theta_i - \psi)$, where ψ is defined in the Eq. (3). Therefore, if $|\theta_i - \psi|$ is small enough, $\theta_i - \psi = \frac{1}{\epsilon k_i}(\omega_i - \Omega)$, and $(\theta_i - \theta_j)^2$ is described as

$$(\theta_i - \theta_j)^2 = \frac{(\omega_i - \Omega)^2}{\epsilon^2 {k_i}^2} + \frac{(\omega_j - \Omega)^2}{\epsilon^2 {k_j}^2} - \frac{2(\omega_i - \Omega)(\omega_j - \Omega)}{\epsilon^2 k_i k_j}, \tag{8}$$

for a set of $\{\omega_i\}$. $\langle S_{ij} \rangle$ is obtained as averaged $(\theta_i - \theta_j)^2$ across a large number of sets of $\{\omega_i\}$. As in the above-described numerical estimation, we assume that $\{\omega_i\}$ is distributed according to the normal distribution with a mean of ω_0 and a standard deviation of σ, and that the synchronized frequency is always Ω in every set of $\{\omega_i\}$. Because we can also assume that ω_0 is nearly equal to Ω, $\langle (\omega_i - \Omega)^2 \rangle$ is considered to be equal to σ^2, and $\langle (\omega_i - \Omega)(\omega_j - \Omega) \rangle$ is considered to be equal to zero. Consequently, we obtain the approximation of $\langle S_{ij} \rangle$ as follows:

$$\langle \tilde{S_{ij}} \rangle = \frac{\sigma^2}{\epsilon^2}(\frac{1}{{k_i}^2} + \frac{1}{{k_j}^2}). \tag{9}$$

This approximation was validated through comparison of $\langle \tilde{S_{ij}} \rangle$ with the real $\langle S_{ij} \rangle$, as shown in Fig. 4 A ($\sigma = 1, \epsilon = 0.3$). The two parameters had a large negative value of Pearson's correlation coefficient (-0.88).

This expression of $\langle \tilde{S_{ij}} \rangle$ implies the reason why the rewiring-based optimization transforms the initial networks to the networks with a rich-club topology: To achieve a small amount of $\langle S \rangle$, $\langle \tilde{S_{ij}} \rangle$ should be small. When the node i already has a high degree in the initial network,

it makes more contribution to a smaller $\langle \tilde{S_{ij}} \rangle$ for the high-degree node to connect with another high-degree node. It is also the case when the node i already has a small degree in the initial network. As a result, during the rewiring, the low-degree nodes are likely to lose their edges, while the high-degree nodes are not. Consequently, high-degree nodes tend to be gathered and create a densely-connected core module, and the remaining low-degree nodes tend to connect with high degree nodes in the core module.

Note that it is difficult to further extend this approximation. If this approximation of $\langle S_{ij} \rangle$ is accurate enough, a simple calculation of Eq. 9 leads us to the proportional relationship between $\langle S \rangle$ and $\frac{1}{\langle k \rangle} \left\langle \frac{1}{k} \right\rangle$. Given $\langle k \rangle$ is a constant value as in the present study, $\langle S \rangle$ should be proportional to $\left\langle \frac{1}{k} \right\rangle$. However, as shown in Fig. 4 B, we could not observe a linear relationship between them. This inaccurate approximation of $\langle S \rangle$ may be caused by accumulation of the small difference between $\langle S_{ij} \rangle$ and $\langle \tilde{S_{ij}} \rangle$. This result suggests that we cannot extend this approximation to representation of $\langle S \rangle$ only by $\left\langle \frac{1}{k} \right\rangle$. In addition, we have to stress that this approximation only hints a possible interpretation on the relationship between the rewiring-based optimization and the rich-club topology, but does not directly explain why networks with the minimum synchronization cost have the rich-club topology.

Acknowledgments

The author thanks Dr. Naoki Masuda for his supports and comments. The author also thanks anonymous reviewers for their helpful suggestions. The author acknowledges the support from the Japan Society for the Promotion of Science (JSPS) Research Fellowship for Young Scientists (222882).

---

[1] O. I. Elgerd, *Electric energy systems theory* (McGraw-Hill Companies, 1982); P. S. Kundur, *Power system stability and control* (McGraw-Hill Companies, 1993).

[2] F. Dörfler and F. Bullo, American Control Conference 2010, 930-937 (2010).

[3] F. Varela, J.P. Lachaux, E. Rodriguez, and J. Martinerie, Nat Rev Neurosci. **2(4)**:229-39 (2001).

[4] J. Fell, and N. Axmacher, Nat Rev Neurosci. **12(2)**:105-18 (2011).

[5] M. Stopfer, S. Bhagavan, B.H. Smith, and G. Laurent, Nature. **390(6655)**:70-4 (1997).

[6] G. Tononi, and G.M. Edelman, Brain Res Brain Res Rev. **31(2-3)**:391-400 (2000).

[7] D.J. Hill, and G. Chen, IEEE Int. Symposium on Circuits and Systems 711-715 (2006).

[8] H. Gharavi, and R. Ghafurian, Proceedings of the IEEE **99**, 917-921 (2011); G.W. Arnold, *ibid.* **99**, 922-927 (2011).

[9] Energy Future Coalition, Report of Smart Grid Working Group, (2008).

[10] S.L. Bressler, R. Coppola, and R. Nakamura, Nature. **366(6451)**:153-6 (1993).

[11] R.D. Traub, M.A. Whittington, I.M. Stanford, and J.G. Jefferys, Nature. **383(6601)**:621-4 (1996).

[12] P.R. Roelfsema, A.K. Engel, P. König, and W. Singer, Nature. **385(6612)**:157-61 (1997).

[13] W.H. Miltner, C. Braun, M. Arnold, H. Witte, E. Taub. Nature. **397(6718)**:434-6 (1999).

[14] J.F. Hipp, A.K. Engel, and M. Siegel, Neuron. **69(2)**:387-96, (2011).

[15] T. Womelsdorf, J-M. Schoffelen, R. Oostenveld, W. Singer, R. Desimone, A.K. Engel, and P. Fries, Science. **316(5831)**:1609-12 (2007).

[16] P. Fries, Trends Cogn Sci (Regul Ed). **9(10)**:474-80 (2005).

[17] A.E. Motter, C. Zhou, and J. Kurths, Phys. Rev. E **71**, 016116 (2005).

[18] T. Nishikawa, and A.E. Motter, Physica D **224**, 77-89 (2006).

[19] M. Brede, Eur. Phys. J. B. **62**, 87-94 (2008).

[20] A. Arenas, A. Diaz-Guilera, J. Kurths, Y. Moreno, and C. Zhou, Phys. Rep. **469**, 93-153 (2008).

[21] L. Buzna, S. Lozano, and A. Diaz-Guilera, Phys. Rev. E **80**, 066120 (2009).

[22] V. Fioriti, S. Ruzzante, E. Castorini, E. Marchei, and V. Rosato, Critical Information Infrastructure Security 14-23 (2009).

[23] M. Breakspear, S. Heitmann, and A. Daffertshofer, Front. Hum. Neurosci. **4**:190 (2010).

[24] J. Gómez-Gardeñes, G. Zamora-López, Y. Moreno, and A. Arenas. PLoS ONE. **5(8)**:e12313 (2010).

[25] L. Donetti, P.I. Hurtado, and M.A. Muñoz, Phys. Rev. Lett. **95**, 188701 (2005).

[26] S. Zhou, and R. Mondragon. IEEE Commun Lett. **8(3)**:180-2 (2004).

[27] V. Colizza, A. Flammini, M. Serrano, and A. Vespignani, Nat Phys. **2(2)**:110-5 (2006).

[28] M.P. van den Heuvel, and O. Sporns, Journal of Neuroscience. **31(44)**:15775-86 (2011).

[29] G. Filatrella, A.H. Nielsen, and N.F. Pedersen, Eur. Phys. J. B. **61**, 485-491 (2008).

[30] D.J. Watts and S.H. Strogatz, Nature **393**, 440 (1998).

[31] A.L. Barabási and R. Albert, Science **286**, 5439 (1999).

[32] J. Gómez-Gardeñes, Y. Moreno, and A. Arenas, Phys. Rev. Lett. **98** 034101 (2007), Phys. Rev. E. **75** 066106 (2007).

[33] A. Bunde, and S. Havlin, *Fractals and Disordered System* (Springer Verlag, 1991).

[34] M.E.J. Newman, Phys. Rev. E. **64** 016131 (2001).

[35] S. Maslov and K. Sneppen, Science **296** 910-913 (2002).

[36] M. Wolfson, Review of Income and Wealth **43**, 4 401 (1997).

[37] TE Gorochowski, M di Bernardo, CS Grierson. Phys Rev E. **81** 056212 (2010).

[38] T. Nishikawa, A.E. Motter, Y.C. Lai, and F.C. Hoppensteadt, Phys. Rev. Lett. **91**, 014101 (2003).

[39] P. Holme, Phys. Rev. E **66**, 036119 (2002).

[40] R. Guimerà, L. Danon, A. Diaz-Guilera, F. Giralt, and A. Arenas, Phys. Rev. E **68**, 065103 (2003).

[41] E. Bullmore, and O. Sporns, Nat Rev Neurosci. 336-349, (2012).

[42] G. Paul, S. Sreenivasan, S. Havlin, and H.E. Stanley, Physica A. **370(2)**:854-62 (2006).

FIG. 1: (Color online) **A**. Main panel: Change of the synchronization cost, $\langle S \rangle$, during rewiring-based optimization. Despite different initial networks (ER, BA, and WS models) with $N = 50, \langle k \rangle = 4$, the synchronization cost converge to a similar amount of $\langle S \rangle$. Sub panel: Change of the standard order parameter, r, during the optimization. In contrast to $\langle S \rangle$, the standard order parameter does not show notable change, just fluctuating below 1. The line shows the change of r when the initial network is the BA model. In cases of the other two initial networks, the similar fluctuations were observed. **B**. Network topology optimized from different initial networks. Optimized networks are similar to each other. They have rich-club network topology, which consists of a densely-connected core module and peripheral low degree nodes connecting with the core. The color in the nodes represent the degree of

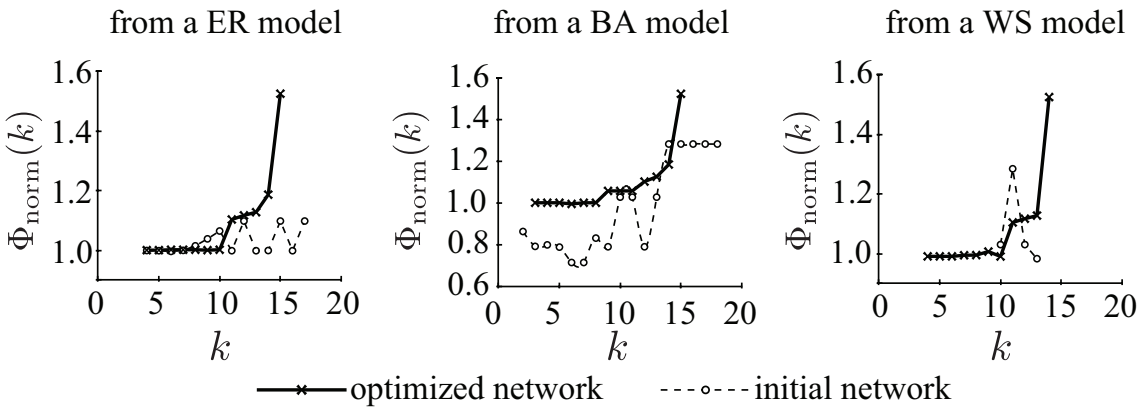

FIG. 2: Difference in rich-club coefficients between the initial networks (circles and dashed lines) and optimized networks (multiple marks and solid lines). While the normalized rich-club coefficients $\Phi_{\rm norm}(k)$ do not show monotonic increase in the initial networks, those in the optimized networks almost monotonically increase. These results suggest that the rewiring-based optimization transforms the initial networks to the networks with a rich-club topology. To clarify the difference between before and after optimization, we adopted larger networks ($N = 100, \langle k \rangle = 10$) than in Fig. 1 ($N = 50, \langle k \rangle = 4$).

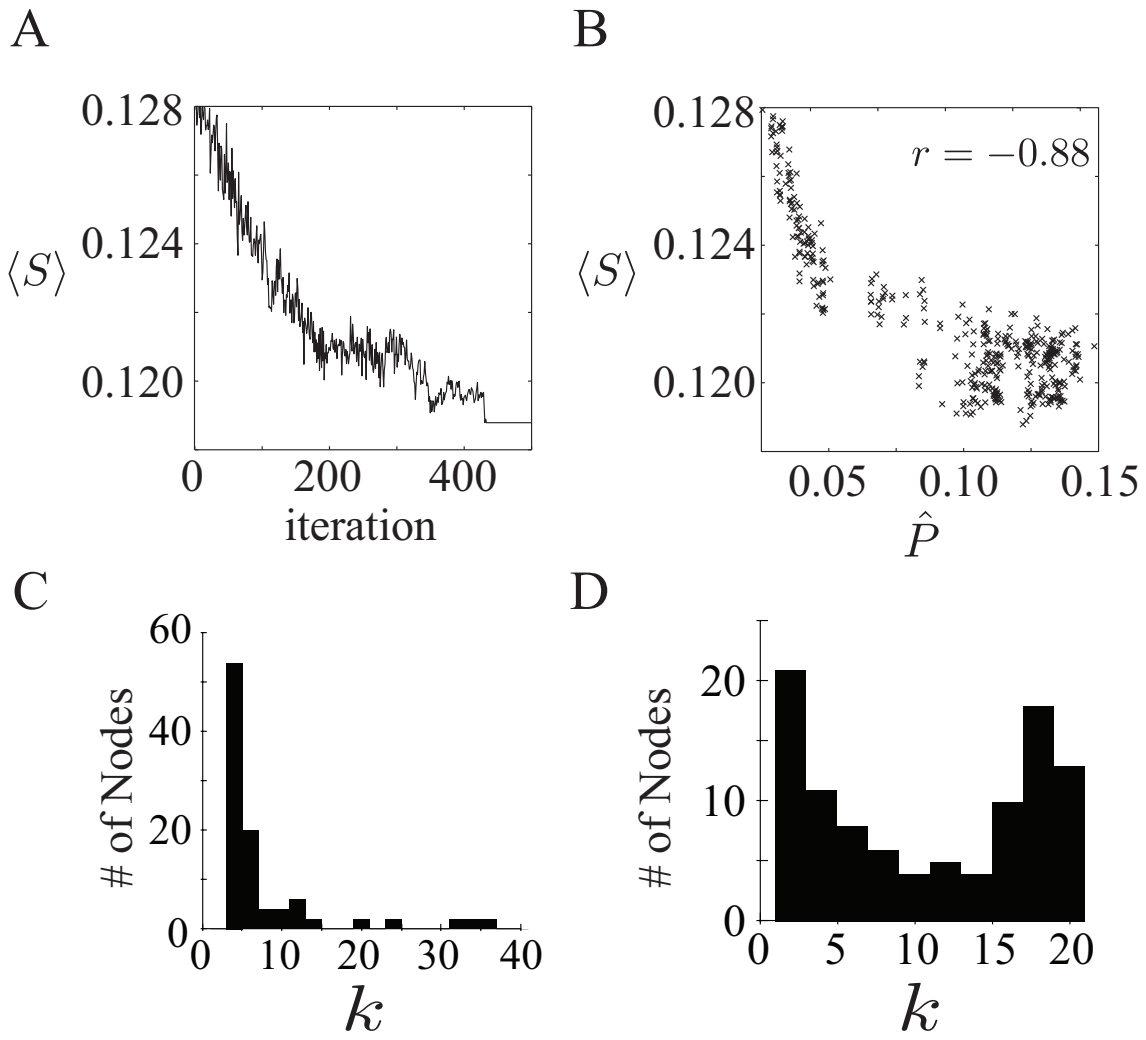

FIG. 3: As the synchronization cost, $\langle S \rangle$, decreases in the rewiring-based optimization (panel **A**), the Wolfson's polarization index, $\hat{P}$, increases (panel **B**). This relation suggests that the rich-club network with a small amount of the synchronization cost can be characterized by bimodal degree distribution, which is quantified by Wolfson's polarization index. Indeed, the degree distribution changed from a power-law distribution (panel **C**) to a bimodal distribution (panel **D**). To clarify the difference between before and after optimization, we adopted larger networks ($N = 100, \langle k \rangle = 4$) than in Fig. 1 ($N = 50, \langle k \rangle = 4$).

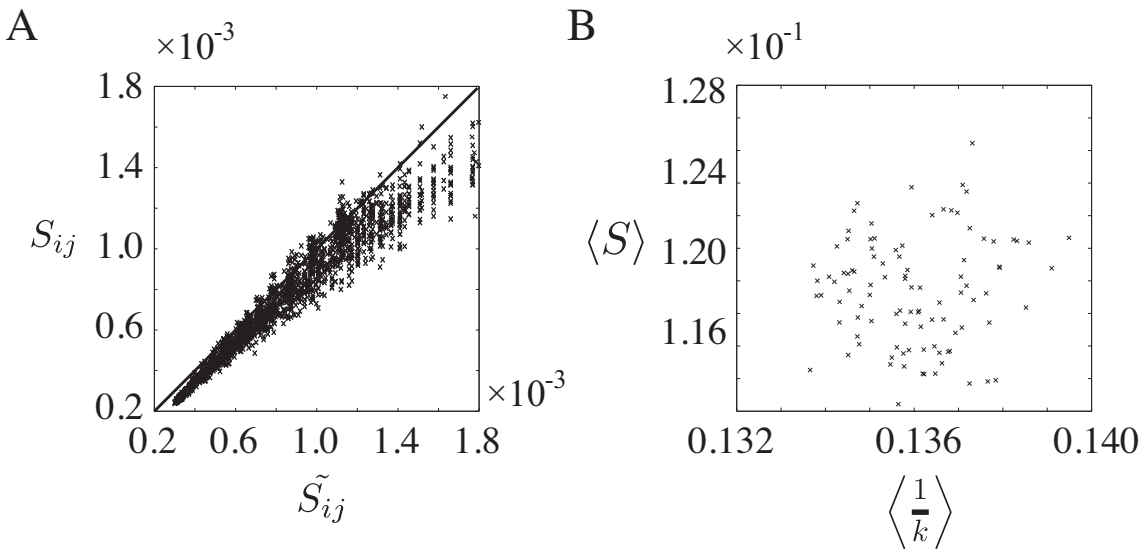

FIG. 4: **A** The analytical approximation of synchronization cost, $\langle \tilde{S_{ij}} \rangle$, is predictive of the real synchronization cost, $\langle S_{ij} \rangle$, in the BA model with $N = 200, \langle N \rangle = 10$. **B** Simple calculations using $\langle \tilde{S_{ij}} \rangle$ suggest a positive linear relationship between $\langle S \rangle$ and $\left\langle \frac{1}{k} \right\rangle$. However, there is not a strong correlation between them, which suggests a limitation of the approximation.

TABLE I: Basic topological properties of the optimized networks. Despite different initial networks, the optimized networks had similar network topological properties. The values for the initial networks represent averaged values across ten estimations, whereas the values for the optimized networks show the mean ± s.d. across the ten estimations.

	$\langle \ell \rangle$		$\langle C \rangle$		$\langle b \rangle$		$r_{\text{assortative}}$	
	initial	optimized	initial	optimized	initial	optimized	initial	optimized
From ER models	1.9	3.5 ± 0.025	0.21	0.13 ± 0.010	44	122.2 ± 3.7	0.034	0.25 ± 0.12
From BA models	1.8	3.3 ± 0.021	0.33	0.15 ± 0.012	48	113 ± 2.8	-0.15	0.28 ± 0.021
From WS models	2.3	3.1 ± 0.017	0.62	0.16 ± 0.010	63	105 ± 2.4	0.047	0.25 ± 0.011

Appendix A: Definition of Synchronization Cost

In this section, we explain why power loss consumed in the electric line between power plants can be represented by square of difference in phase of voltage between the two power plants.

In the following model, as in previous studies [2, 22], we do not consider the effect of the length of the power line on the power loss. To estimate the power loss in a typical power line shown in Fig. 5, we estimate active power flow (P_{ij} and P_{ji}), reactive power flow (Q_{ij} and Q_{ji}), and delayed reactive power flow (Q_{ci} and Q_{cj}) as follows [1]:

$$P_{ij} = \frac{V_i V_j \sin(\theta_i - \theta_j)}{{Z_{ij}}^2 / f_0 L_{ij}} + \frac{{V_i}^2 - V_i V_j \cos(\theta_i - \theta_j)}{{Z_{ij}}^2 / R_{ij}}, \tag{A1}$$

$$Q_{ij} = -\frac{V_i V_j \sin(\theta_i - \theta_j)}{{Z_{ij}}^2 / R_{ij}} + \frac{{V_i}^2 - V_i V_j \cos(\theta_i - \theta_j)}{{Z_{ij}}^2 / f_0 L_{ij}}, \tag{A2}$$

$$Q_{ci} = \frac{f_0 C_{ij}}{2} {V_i}^2, \tag{A3}$$

where f_0 represents synchronized angular frequency of alternating voltage, and ${Z_{ij}}^2 = {R_{ij}}^2 + (f_0 L_{ij})^2$. P_{ji}, Q_{ji}, and Q_{cj} are obtained by exchanging i and j. Using these power flows, the active power loss due to resistance, $P^{ij}_{\rm loss}$, is calculated as $P_{ij} + P_{ji}$, whereas the reactive power loss due to inductance, $Q^{ij}_{\rm loss}$, is estimated as $Q_{ij} + Q_{ji} + Q_{ci} + Q_{cj}$ as follows:

$$P^{ij}_{\rm loss} = \frac{R_{ij}}{{Z_{ij}}^2} \left(-2 V_i V_j \cos(\theta_i - \theta_j) + {V_i}^2 + {V_j}^2 \right), \tag{A4}$$

$$Q^{ij}_{\rm loss} = \frac{{Z_{ij}}^2}{f_0 L_{ij}} \left(-2 V_i V_j \cos(\theta_i - \theta_j) + {V_i}^2 + {V_j}^2 \right) + \frac{f_0 C_{ij}}{2} ({V_i}^2 + {V_j}^2). \tag{A5}$$

The total power loss is estimated as a combination of the active power loss and the reactive power loss [1]. By using a second-order Taylor expansion, we regard the total power loss, $P^{ij}_{\rm loss} + Q^{ij}_{\rm loss}$, as $a_0 + a_1 (\theta_i - \theta_j)^2$, where a_0 and a_1 are constants ($a_1 > 0$). Therefore, we define the synchronization cost, S_{ij}, for a power line between power plants i and j as

$$S_{ij} = (\theta_i - \theta_j)^2 . \tag{A6}$$

Appendix B: Power Grid as Kuramoto Model

In this section, we explain that, under several assumptions, we can approximate power grids by the first-order Kuramoto model of nonuniform oscillators.

As previous studies [2, 21, 22], we model a power grid as follows: The structure of the power grid with N power plants is represented as an unweighted and undirected adjacency matrix A,

where a node represents a power plant and an edge a power line. A_{ij} is 1 when power plants i and j have a power line between them, and A_{ij} is 0 when they do not. According to the previous studies [2, 21, 22], the phase of the output voltage of the power plant i, θ_i, is described as

$$\dot{\theta}_i = \frac{f_i}{D_i} - \sum_j \frac{W_{ij}}{D_i} A_{ij} \sin(\theta_i - \theta_j), \tag{B1}$$

where D_i denotes a damping constant, W_{ij} is an amount of power transfer between power plants i and j, and f_i represents the natural frequency of the output voltage from the power plant i. To reduce computational cost for the following rewiring-based optimization, we assume that $W_{ij}/D_i = \epsilon$ for any power line. Because f_i/D_i is specific to power plant i, we replace the value with ω_i. Consequently, the voltage phase of the power plants can be expressed in the Kuramoto model as

$$\dot{\theta}_i = \omega_i - \epsilon \sum_j A_{ij} \sin(\theta_i - \theta_j). \tag{B2}$$

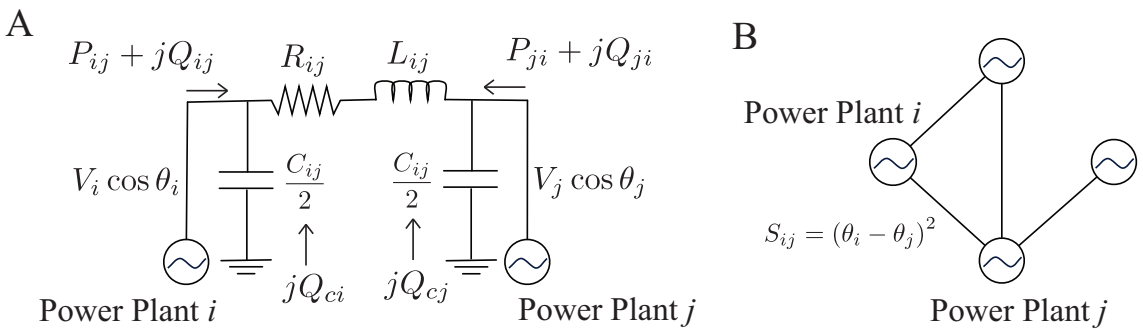

FIG. 5: Panel **A** shows a typical power line between power plants i and j. $V_i \cos\theta_i$ and $V_j \cos\theta_j$ indicate the voltage of the output from the power plants. R_{ij}, L_{ij}, and C_{ij} indicate resistance, inductance, and conductance between the power plants. As show in panel **B**, S is defined in every power line based on the phase difference of the voltages between the connecting power plants.